



Microcompression of Bulk Metallic Glass and Tungsten – Bulk Metallic Glass Composites

**by Brian E. Schuster, Lee S. Magness, Laszlo J. Kecskes, Qiuming Wei,
Michael K. Miller, Matthew H. Ervin, Stephan Hruszkewycz,
Todd C. Hufnagel, and Kaliat T. Ramesh**

ARL-RP-178

May 2007

A reprint from the Proceedings of the 25th Army Science Conference, Orlando, FL, 27–30 November 2006.

NOTICES

Disclaimers

The findings in this report are not to be construed as an official Department of the Army position unless so designated by other authorized documents.

Citation of manufacturer's or trade names does not constitute an official endorsement or approval of the use thereof.

Destroy this report when it is no longer needed. Do not return it to the originator.

Army Research Laboratory

Aberdeen Proving Ground, MD 21005-5069

ARL-RP-178**May 2007**

Microcompression of Bulk Metallic Glass and Tungsten – Bulk Metallic Glass Composites

Brian E. Schuster, Lee S. Magness, and Laszlo J. Kecskes
Weapons and Materials Research Directorate, ARL

Qiuming Wei
University of North Carolina

Michael K. Miller
Oak Ridge National Laboratory

Matthew H. Ervin
Sensors and Electron Devices Directorate, ARL

Stephan Hruszkewycz, Todd C. Hufnagel, and Kaliat T. Ramesh
Johns Hopkins University

A reprint from the Proceedings of the 25th Army Science Conference, Orlando, FL, 27–30 November 2006.

REPORT DOCUMENTATION PAGE				Form Approved OMB No. 0704-0188	
Public reporting burden for this collection of information is estimated to average 1 hour per response, including the time for reviewing instructions, searching existing data sources, gathering and maintaining the data needed, and completing and reviewing the collection information. Send comments regarding this burden estimate or any other aspect of this collection of information, including suggestions for reducing the burden, to Department of Defense, Washington Headquarters Services, Directorate for Information Operations and Reports (0704-0188), 1215 Jefferson Davis Highway, Suite 1204, Arlington, VA 22202-4302. Respondents should be aware that notwithstanding any other provision of law, no person shall be subject to any penalty for failing to comply with a collection of information if it does not display a currently valid OMB control number. PLEASE DO NOT RETURN YOUR FORM TO THE ABOVE ADDRESS.					
1. REPORT DATE (DD-MM-YYYY) May 2007		2. REPORT TYPE Reprint		3. DATES COVERED (From - To) 30 September 2005–30 September 2006	
4. TITLE AND SUBTITLE Microcompression of Bulk Metallic Glass and Tungsten – Bulk Metallic Glass Composites				5a. CONTRACT NUMBER	
				5b. GRANT NUMBER	
				5c. PROGRAM ELEMENT NUMBER	
6. AUTHOR(S) Brian E. Schuster, Lee S. Magness, and Laszlo J. Kecskes, Qiuming Wei, [*] Michael K. Miller, [†] Matthew H. Ervin, Stephan Hruszkewycz, [‡] Todd C. Hufnagel, [‡] and Kaliat T. Ramesh [‡]				5d. PROJECT NUMBER 68T2G1	
				5e. TASK NUMBER	
				5f. WORK UNIT NUMBER	
7. PERFORMING ORGANIZATION NAME(S) AND ADDRESS(ES) U.S. Army Research Laboratory ATTN: AMSRD-ARL-WM-TC Aberdeen Proving Ground, MD 21005-5069				8. PERFORMING ORGANIZATION REPORT NUMBER ARL-RP-178	
9. SPONSORING/MONITORING AGENCY NAME(S) AND ADDRESS(ES)				10. SPONSOR/MONITOR'S ACRONYM(S)	
				11. SPONSOR/MONITOR'S REPORT NUMBER(S)	
12. DISTRIBUTION/AVAILABILITY STATEMENT Approved for public release; distribution is unlimited.					
13. SUPPLEMENTARY NOTES A reprint from the <i>Proceedings of the 25th Army Science Conference</i> , Orlando, FL, 27–30 November 2006. [*] University of North Carolina, Mechanical Engineering Department, Charlotte, NC 28223 [†] Oak Ridge National Laboratory, Materials Science and Technology Division, Oak Ridge, TN 37831 [‡] The Johns Hopkins University, Baltimore, MD 21218					
14. ABSTRACT Recently, there has been tremendous interest in the size-dependent mechanical properties of materials, in particular, using various applications of the micrometer-scale uniaxial compression technique. In this technique, site-specific focused ion beam (FIB) milling is employed to fabricate micrometer sized compression specimens (micro-posts) from otherwise bulk material. These micro-posts are then tested in uniaxial compression using a flat punch indenter in a conventional nanoindenter. We apply this technique to examine the mechanical properties of bulk metallic glass (BMG) systems from two perspectives; micro-electro-mechanical systems, and tungsten (W)-BMG composite kinetic energy penetrators (KEP). The mechanical properties of Pd ₄₀ Ni ₄₀ P ₂₀ are found to be relatively free from scale effects approaching the micron size scale. There are, however, moderate increases in strength for micrometer sized, likely resulting from extrinsic factors such as local heterogeneities, pores, and/or other defects are able to act as points of stress concentrations. While the mechanical properties of monolithic amorphous alloys are well understood, local heterogeneities in W-BMG composites may affect the response of the composite. With this motivation, the micro-posts of the BMG are machined from the composite material using site-specific FIB milling. The mechanical properties of the BMG matrix are examined, and thus microcompression is used as a tool to relate local mechanical properties to the expected bulk response in these composites.					
15. SUBJECT TERMS metallic glass, MEMS, nanoindenter, shear bands, mechanical properties					
16. SECURITY CLASSIFICATION OF:			17. LIMITATION OF ABSTRACT UL	18. NUMBER OF PAGES 13	19a. NAME OF RESPONSIBLE PERSON Brian E. Schuster
a. REPORT UNCLASSIFIED	b. ABSTRACT UNCLASSIFIED	c. THIS PAGE UNCLASSIFIED			19b. TELEPHONE NUMBER (Include area code) 410-278-6733

Microcompression of Bulk Metallic Glass and Tungsten - Bulk Metallic Glass Composites

Brian E. Schuster*, Lee S. Magness, Laszlo J. Kecskes
Weapons and Materials Research Directorate, Army Research Laboratory
AMSRD-ARL-WM-TC, Aberdeen Proving Ground, MD 21005-5069

Qiuming Wei
University of North Carolina at Charlotte, Mechanical Engineering Department
Charlotte, NC 28223

Michael K. Miller
Materials Science and Technology Division, Oak Ridge National Laboratory
Oak Ridge, TN 37831

Matthew H. Ervin
Sensors and Electronic Devices Directorate, Army Research Laboratory
Adelphi, MD, 20783

Stephan Hruszkewycz, Todd C. Hufnagel, Kalia T. Ramesh
The Johns Hopkins University
Baltimore, MD 21218

1. INTRODUCTION

Recently, there has been tremendous interest in the size dependent mechanical properties of materials, in particular, using of the micrometer-scale uniaxial compression technique (microcompression). In this technique, focused ion beam (FIB) milling is employed to fabricate micrometer sized compression specimen (micro-posts) from otherwise bulk material. These micro-posts, as shown in figure 1, are then tested in uniaxial compression using a flat punch indenter in a conventional nanoindenter. This technique was first applied to examine the mechanical properties of sub-millimeter sized specimen of single crystals of Ni, single crystal Ni_3Al -1%Ta, a Ni based superalloy and in gold (Uchic et al., 2003, 2004, Greer et al. 2005). These studies recognized that for some materials (other than carefully grown, defect free whiskers), the deformation and mechanical properties were highly dependent on the physical length scale of the specimen. Clearly then, a study of the size dependant mechanical properties is crucial for designing devices on a like scale. In other applications, this technique is a powerful tool for examining the mechanical properties of specimen that are ill-suited for traditional mechanical testing. For example, this technique has been applied to examine the compressive properties of electrodeposited nanocrystalline Ni (Schuster et al., 2006), a material examined in detail in tension and indentation. Because of limited thickness, this material does not lend itself to traditional compression testing. With the site-specific nature of specimen production using a FIB, it is also possible to isolate individual phases in a material and

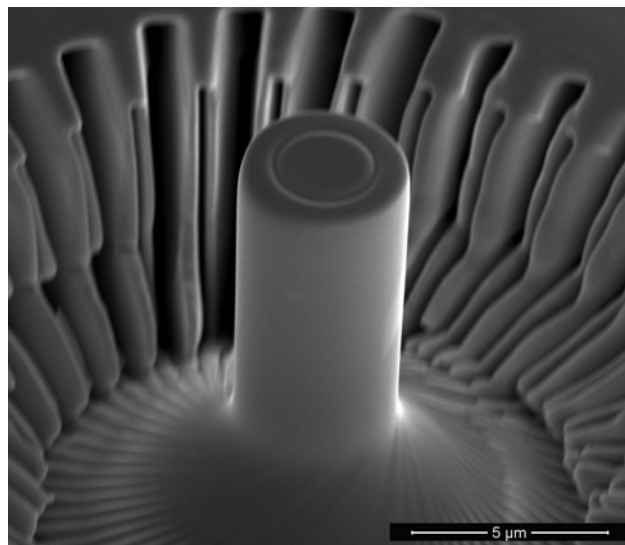


Fig. 1. A 5 μm diameter microcompression specimen of $\text{Pd}_{40}\text{Ni}_{40}\text{P}_{20}$ fabricated by FIB machining.

measure their individual response, with the eventual goal of relating bulk properties to the behavior of its micro-scale constituents.

There has been keen interest in thin film metallic glass (TFMG) and BMG within micro-electro-mechanical systems (MEMS) as these materials are regarded to be isotropic and homogeneous, with relatively size independent mechanical properties. Processing in the supercooled liquid region (SCLR) allows for replication of micron and sub-micron features using warm pressing

of Si based MEMS devices and even more complex 3D forms such as spring actuators (Lewandowski et al., 2006, Hata et al., 2003). The ability to fabricate these small-scale structures must come with an understanding of mechanical properties at a like scale. In contrast to some single crystal systems, it has been assumed that these mechanical properties will be relatively free from scale effects approaching the micron size scale, as the intrinsic deformation mechanisms operate on a much finer scale.

BMG materials have also been investigated for use in kinetic energy penetrator applications. These materials possess tremendous strength, low strain hardening, and low heat capacity and are therefore prone to adiabatic shear band (ASB) formation during ballistic impacts. This ASB formation during ballistic impact of long rod penetrators has been shown to induce the self sharpening deformation mechanism responsible for the superior performance of certain depleted uranium alloys when compared to tungsten heavy alloys (Magness and Farrand 1990). Similarly, tungsten (W) – BMG composites have been investigated for penetrator applications in the hope that this failure mechanism can be retained for composite materials in deep penetration events.

While the mechanical properties and deformation mechanisms of monolithic BMG in bulk form are generally well understood, these properties are not necessarily equivalent for the BMG alloys cast in composite form or for that matter, necessarily equivalent in micro-scale specimens. For W-BMG composites, dissolution of W in the BMG matrix is frequently manifested in the formation of complex crystalline phases which thereby decrease the overall amorphous content of the matrix. It is then important to compare the properties and deformation mechanisms of the monolithic alloys with the Hf alloy as found in the composite, with the presence other phases and heterogeneities.

In this paper, the mechanical properties of BMG materials are investigated using microcompression. This technique is applied to two BMG systems; monolithic $\text{Pd}_{40}\text{Ni}_{40}\text{P}_{20}$ and a composite of a Hf based BMG infiltrated into a porous tungsten precursory form (preform). For the W-BMG composites, microcompression is applied as a diagnostic tool in examining the properties of this Hf-based matrix after it has been incorporated to form the composite. Do these materials retain characteristics that make them susceptible to ASB formation including high strength and low strain hardening? Any assessment at the micrometer scale must be coupled with an understanding of the dependence of properties on specimen dimension. For example, is the measured strength an artifact of specimen size or a description of the intrinsic behavior? To strengthen this understanding, bulk and micrometer sized $\text{Pd}_{40}\text{Ni}_{40}\text{P}_{20}$

specimens are examined in compression to investigate the size dependence (or lack thereof) on deformation.

2. EXPERIMENTAL

$\text{Pd}_{40}\text{Ni}_{40}\text{P}_{20}$ ingots were prepared by induction melting Pd and Ni_2P powders in an argon atmosphere in a quartz tube (Kui et al., 1984). W-BMG composite materials were prepared by Liquidmetal® Technologies by infiltrating a porous tungsten “preform” with a proprietary Hf-based BMG matrix. A back-scattered Scanning Electron Microscope (SEM) micrograph of the typical two-phase microstructure of the W-BMG is shown in figure 2. The W phase (lighter phase) makes up a majority of the volume fraction of the composite, while the Hf-BMG (darker phase) forms a continuous three-dimensional network as a matrix.

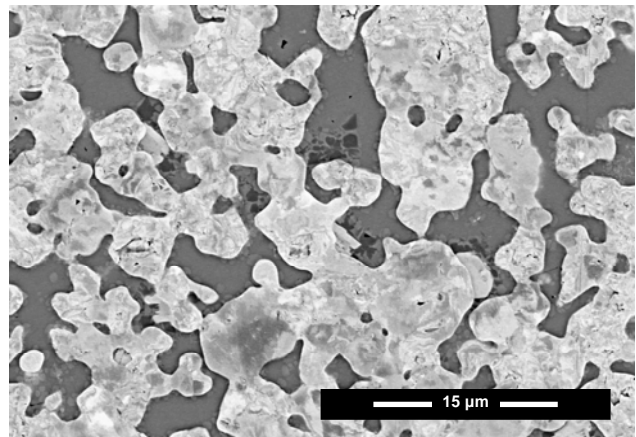


Fig. 2. A backscattered SEM micrograph of a typical W-BMG composite material fabricated by liquid infiltration of a Hf-based BMG matrix (darker phase) into a porous W preform (light phase).

Platens of each material were lapped flat and parallel while polished to a final sub-micron finish. Micro-posts were prepared via FIB milling in an FEI Nova 600. Initially, the ion beam was oriented normal to the plane of the bulk specimen and high currents of 7 to 20 nA were used to milled out the precursory forms of the specimen. Final “lathe” milling was performed with the ion beam inclined to an angle of 52° with respect to the pillar axis for final machining at 100-1000 pA. The sample is incrementally machined to a specified height and diameter using sample rotations of 5 to 10°. This technique, explained in detail by Uchic et al. (2005), was applied to fabricate specimens of $\text{Pd}_{40}\text{Ni}_{40}\text{P}_{20}$ with diameters ranging from 2 to 10 μm , with aspect ratios (height to diameter ratio) of 2 to 2.5, an example of which is shown in figure 1. Because of the limited size of individual “pools” of the BMG material in the composites and the desire to isolate the response of the Hf based

BMG matrix, micro-posts from the W-BMG composites, as shown in figure 3, were limited to $\sim 4\mu\text{m}$ in diameter.

Micro-posts from the monolithic $\text{Pd}_{40}\text{Ni}_{40}\text{P}_{20}$ and the W-BMG composite material were then tested in microcompression in an MTS Nanoindenter XP with Continuous Stiffness Measurement, while bulk samples (of $\text{Pd}_{40}\text{Ni}_{40}\text{P}_{20}$) were deformed in an MTS servo-hydraulic loading system. The micro-posts were deformed using a flat punch indenter with a square cross-section of $35\mu\text{m} \times 35\mu\text{m}$; an indenter that is much larger in cross-section than the micro-posts and therefore loading the specimen in uniaxial compression. Using a custom method for Testworks 4.0, the loading rate in these load-controlled experiments was specified to obtain nominal strain rates of $10^{-4}/\text{s}$. The specimen load and cross-head displacement are recorded with nano-newton and sub-nanometer resolution respectively. The specimens are deformed to a specified displacement (or strain) followed by an incremental unloading. Specimen dimensions prior to deformation are measured from high resolution SEM micrographs of the micro-posts captured prior to deformation and through automated image analysis in Image Pro Plus 5.0. Specimen stress and strain are calculated in the same manner as a traditional compression test using the initial specimen dimensions and the load/displacement data.

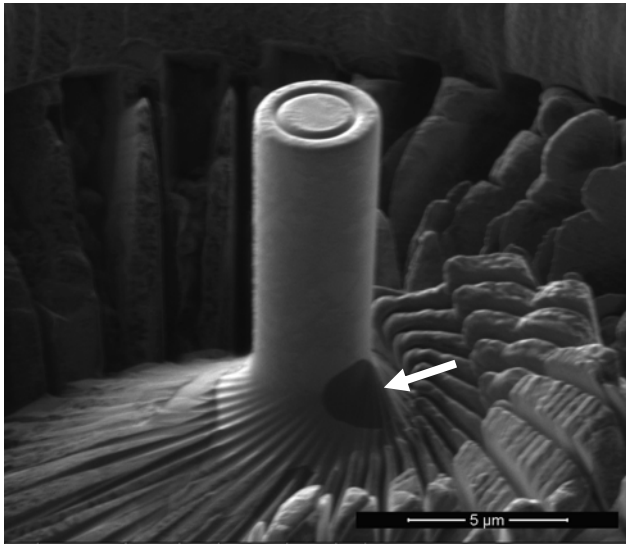


Fig. 3. An ion beam micrograph of a $4.2\mu\text{m}$ micro-post machined from the W-BMG composite material. With the exception of a single W particle at the base (as indicated by an arrow), this micro-post consists only of the Hf-based matrix (Note: In the ion beam micrograph, the contrast is reversed with the W phase appearing as the darker phase).

3. RESULTS AND ANALYSIS

3.1 Results for $\text{Pd}_{40}\text{Ni}_{40}\text{P}_{20}$

Bulk samples of $\text{Pd}_{40}\text{Ni}_{40}\text{P}_{20}$ showed average yield strength of 1.78 GPa, a value that matches well with that measured by Wright et al.¹³. The calculated engineering stress-strain curves from the microcompression tests are shown in figure 4(a). On average, these BMG micro-posts are found to load to an average 0.2% offset yield strength of 1.95 GPa, an increase of roughly 10% over the bulk counterparts; a moderate but significant increase.

Because of the fixed base geometry of microcompression, this technique is in general not well suited for accurate measure of the elastic modulus of the material. The specimen base adds an additional compliance to the system that effectively lowers the measured Young's modulus of the material (Zhang et al., 2006). In finite element analyses of the effect of the elastic base on the measured response for specimens with a 128° contact angle, the measured elastic modulus was approximately 80% of the actual elastic modulus. In this study, the average measured modulus was 68 GPa. In correcting for the base compliance of the materials, this suggests an average Young's modulus of 86 GPa. This value is somewhat lower than that found elsewhere (Wright et al., 2001), though any difference may be attributed to misfit/misalignment as a misalignment of 1° may decrease the measured modulus by 20% (Zhang et al., 2006).

In $\text{Pd}_{40}\text{Ni}_{40}\text{P}_{20}$, the stress-strain graphs from microcompression have obvious differences from bulk counterparts. Typically in the compressive deformation of BMG's, many shear band events occur prior to the failure. This "serrated" flow phenomena has been carefully examined bulk samples of $\text{Pd}_{40}\text{Ni}_{40}\text{P}_{20}$ system (Wright et al., 2001). In displacement driven bulk tests, there is a clear drop in the specimen load associated with shear band events as the load is relaxed as the specimens begin to permanently deform (Wright et al., 2001). Even at a specimen size of several micrometers found in this study, serrated flow is apparent and is characterized by sudden strain bursts at a constant applied stress, much like a dead weight during deformation. These "pop-in" events correspond to localized deformation along shear bands. As an example, consider the stress-strain plot for the $4.43\mu\text{m}$ specimen found in figure 4(a); a large strain burst of 250 nm is observed, followed by complete unloading of the specimen. It is not immediately obvious if this strain burst is a result of a single or multiple shear band events. This sample was examined with an SEM and this strain burst was in fact associated with the formation as many as 5 separate shear bands with multiple intersecting branches, as shown in figure 5(a). A subsequent

reloading showed that this previously deformed specimen was still able to sustain a considerable load; a strain burst of ~20 nm at a load of 1.8 GPa and an eventual 0.2% offset yield point of 1.98 GPa. Even this sample with multiple shear bands propagating across the specimen is able to support the same load as in the undeformed state.

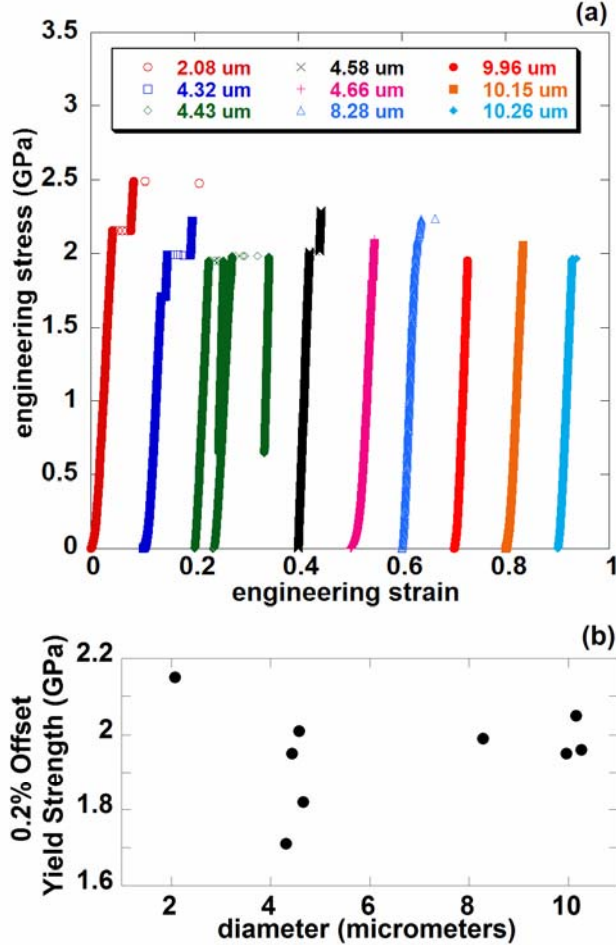


Fig. 4. (a) Engineering stress and strain plots for $\text{Pd}_{40}\text{Ni}_{40}\text{P}_{20}$ specimens varying in size from 2 to 10 μm in diameter (offset for clarity). (b) Plot of 0.2% offset yield strength for all $\text{Pd}_{40}\text{Ni}_{40}\text{P}_{20}$ specimens tested. Overall average yield is found to be 1.95 GPa.

There is a moderate, yet unequivocal increase in yield strength in decreasing from bulk to micro-scale specimens. When comparing any strength variations at the micrometer scale several points of caution should be raised. The 0.2% offset yield strength of specimens with sizes ranging from 2 to 10 μm is shown in figure 4(b). While the yield strength of the ~2 μm sample exceeds that of the rest of the specimens, this does not necessarily indicate a strong dependence in the strength with decreasing specimen size; any moderate increase with decreasing specimen size is on the order of the scatter in the data and therefore should be examined with a more statistical approach. A first glance at figure 4(a) might again give the impression of a moderate increase in

strength with decreasing specimen size as the ultimate engineering strength increases with decreasing specimen size. This increase in peak stress is most likely an artifact of the microcompression test. At times, as in figure 5(b), the deformation along shear bands is accompanied with an increase in the cross-sectional area at the loading surface of the micro-post. The stress strain plot of this 2.08 μm diameter specimen suggests a yield strength of 2.15 GPa and peak compressive strength of 2.5 GPa. Using the final micro-post area at the indenter surface to account for the “true stress” in the material suggests a greatly decreased specimen stress at fracture.

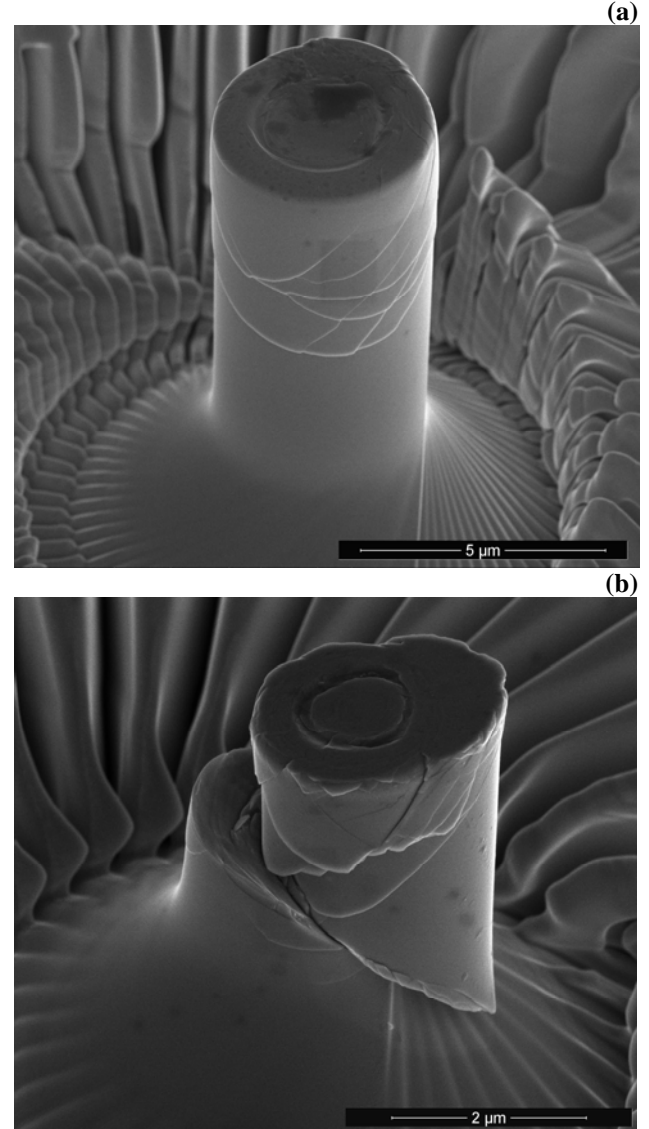


Fig. 5. (a) A deformed 4.43 μm diameter specimen showing multiple shear bands with out failure in loading to 2 GPa (b) A severely deformed 2.08 μm diameter specimen where the resulting shear deformation has resulted in an increased surface area at the loading surface.

Post-mortem SEM analysis provides an opportunity to examine the deformation behavior and perform fractography on the micro-posts. Deformation is typical of that shown in figure 5(a) and (b); permanent deformation is accompanied by the initiation and propagation of multiple shear bands and planes. And whereas the fracture surface of conventional-sized BMG specimen is often accompanied with formation of a river pattern on the fracture surface, these features are not present in the SEM micrograph shown in figure 6. The fracture surface in this specimen appears as a planar fault along a shear band with a very plane/flat morphology. This topology changes dramatically as the specimen undergoes a final-fast fracture and the fracture surface is more faceted in appearance.

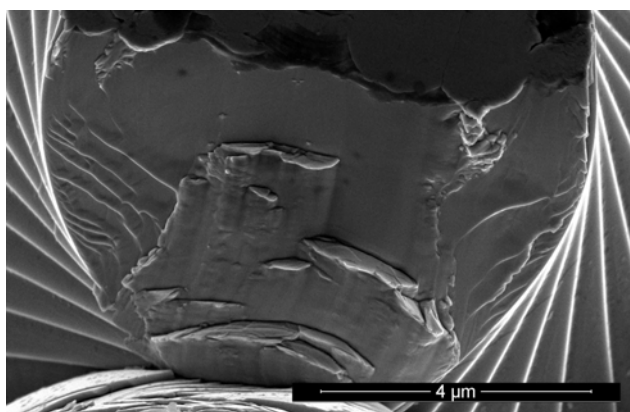


Fig. 6. SEM micrograph of the fracture surface from a failed microcompression specimen.

3.2 Results for W-BMG

The compressive true stress – true strain plots from the Hf-based matrix of the W-BMG matrix are shown in figure 7. The 4.20 μm diameter sample showed a 0.2% offset yield strength of 2.0 GPa and an ultimate compressive strength of 2.68 GPa. After yield at $\sim 3\%$ strain, the material undergoes 5% plastic strain accompanied by considerable strain hardening, in stark contrast to typical monolithic BMG materials. To further investigate the strain hardening behavior, a second specimen was initially loaded beyond the yield strength, unloaded, then reloaded until failure. The true stress – true strain plot for the 3.73 μm diameter specimen shown in figure 7 showed a 0.2 % yield strength of 2.20 GPa. Upon reaching a load of 2.5 GPa, the specimen was unloaded completely. On reloading, the measured 0.2% offset yield strength was 2.5 GPa; the strain hardening was irreversible and deformation commenced when the load exceeded the peak strength from the initial test. The peak strength on the subsequent loading was 2.9 GPa.

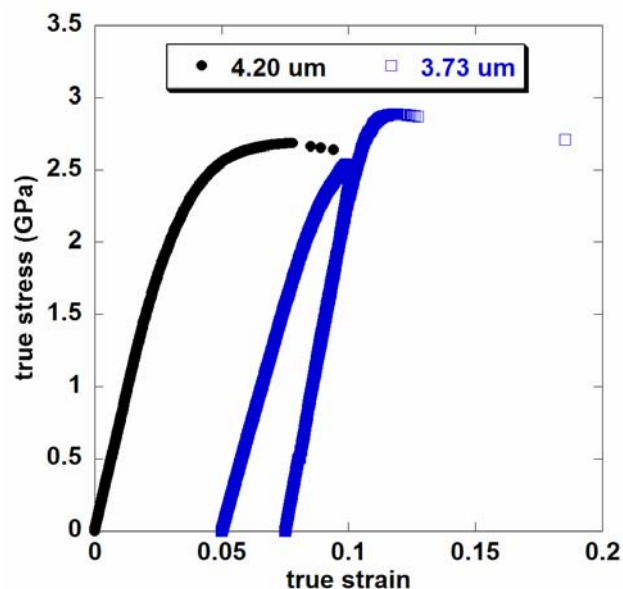


Fig.7. True stress-true strain plots for microcompression specimens cut from a W-BMG matrix specimen. The 3.73 μm specimen was multiply loaded and demonstrates some work hardening.

The fracture surface from the 4.20 μm specimen is shown in figure 8. The fracture surface does demonstrate some ductile features and possibly a failure at the interface between the BMG matrix and a tungsten particle. From this initial view, it is not clear how the fracture may have been affected by any stress concentration at a W-BMG interface. For further insight into the material fracture, this specimen was sectioned via FIB milling. The SEM micrograph of the through section of the fracture surface is shown in figure 8(b). This backscattered SEM micrograph indicates that the material at the fracture surface consists primarily of the Hf-based phase. The W particles at the base of the specimen may have affected the fracture behavior of the micro-post. As the fracture surface does seem to follow parallel to the plane of the W particle near the surface. While microcompression may not be the best experiment to evaluate interface strengths in materials, this test may indicate a strong bond between the phases as this interface seemingly remained intact on failure.

4. DISCUSSION

To review, this study sought to measure the mechanical properties of micrometer sized BMG specimens. Typically, it is assumed that these materials are isotropic, homogeneous and relatively size independent mechanical properties. In addition, this technique has been used to isolate and measure the mechanical properties of the Hf-based matrix of the W-BMG material.

The $\text{Pd}_{40}\text{Ni}_{40}\text{P}_{20}$ showed moderate increases in strength of 10% compared to bulk counterparts. Deformation after yield is characterized by inhomogeneous deformation by the formation of multiple shear bands/planes leading to failure. As expected, there is no evidence of strain hardening in these materials in bulk or micro-scale specimen. On occasion, the deformation occurs by serrated flow, where the flow is characterized by sudden strain bursts at a constant load.

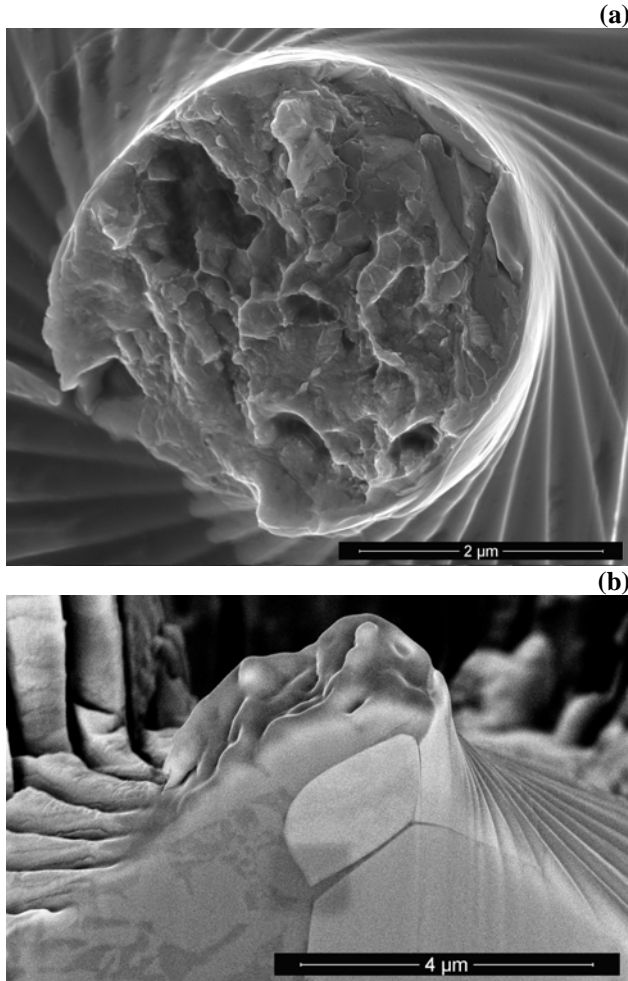


Fig. 8(a) A SEM micrograph of the fracture surface of a 4.20 μm microcompression specimen (see accompanying stress-strain plot in figure 7). (b) SEM of the specimen from (a) that has been sectioned by FIB milling showing a tungsten particle immediately below the fracture surface.

In returning to the hypothesis that BMG and TFMG materials should have “relatively size independent mechanical properties”, an explanation is needed for the moderate increases in strength observed in these micro-posts. Unlike pure fcc single crystals presented in other studies (Uchic et al., 2003, 2004, Greer et al., 2005), the intrinsic deformation mechanisms such as shear transformations zones (STZ) (and collections of STZ's) operate on a much smaller size scale than has been

examined in this study (Lambson et al., 1986). It is therefore unlikely that these processes would be affected by the change in specimen size from the millimeter to micrometer size. It is suggested that other extrinsic factors such as local heterogeneities, pores, and/or other defects act as stress concentrations, leading to the eventual failure in bulk specimens. While not well quantified in this study, pores were found in the polished platen cross-section with diameters ranging from hundreds of nanometers to several tens of micrometers. The largest micro-post examined in this study displaces a volume of roughly $1600 \mu\text{m}^3$. The probability of pores in this limited volume is very small when compared to any bulk specimens of the same material. It is then reasonable to suggest that this decreased defect population, rather than any change in the intrinsic deformation mechanism explains the apparent strength increase.

The deformation of W-BMG specimen does show stark contrasts from the monolithic BMG. The material does seemingly possess tremendous strength at the $\sim 4\mu\text{m}$ size, and the plastic deformation is accompanied by strain hardening of the material. No strain hardening was observable in the Pd glass in specimen ranging in size from several micrometers to millimeters in diameter. In these two tests, there may be some dependence of the flow strength on specimen size as the $3.73\mu\text{m}$ specimen was measurably stronger than the $4.20\mu\text{m}$ specimen, but it is not clear how local variations in the amorphous content and structure could affect the measured response. While the material volume of an individual pool of BMG in these composite materials is very limited, dependence of the strength on size must be examined in more detail. In UM F19, a Ni based superalloy material, size dependence in flow strength below a size of $5\mu\text{m}$ is also accompanied by work hardening, a feature not observed in larger specimens. While this is not a confirmation of the deformation behavior observed in this study, it is important to note any potential test artifacts that could cause variations from the intrinsic deformation behavior of the material. Clearly though, the deformation behavior of this Hf-based BMG in composite form does vary from the ideal shearing behavior of a typical BMG at these specimen sizes and strain rates. Further testing is required to examine parallels in material properties at high/ballistic strain rates. The material still apparently retains a high strength and relatively low strain hardening, important characteristics for penetrator materials.

The interaction of the matrix material and the W particles is an interesting study in itself. The overall composite yield strength could be estimated from the rule of mixtures for the W and BMG matrix. Using an assumed strength for the W phase based on the Hall-Petch relationship and the measured strength of the BMG matrix results in an estimated value of the composite's strength that is within 5~10% of measured values. This is not a

confirmation of the ability to use microcompression to estimate bulk properties, but is an important reality check.

In many other metal matrix composite materials, the strengthening phase is both the stronger and stiffer phase:: e.g. SiC or other ceramic particles used in strengthening Al alloys. In this material, the W particles are stiffer elastically than the Hf based matrix by as much as 4:1, but this matrix is tremendously stronger. The effect of this interaction on the bulk response should be investigated as it would affect the composites susceptibility to ASB formation, composite strength and ductility. A path for future studies could include an evaluation of the properties of both the W and the matrix phase. Size effects in the bcc W could be a complicating factor in the analysis. This behavior has been addressed for fcc gold and nickel ((Uchic et al., 2003, 2004, Greer et al., 2005), but has not been investigated for tungsten or any bcc materials.

5. CONCLUSION

Micro-scale uniaxial compression has been used to examine the mechanical properties of a monolithic BMG and a W-BMG composite. In $\text{Pd}_{40}\text{Ni}_{40}\text{P}_{20}$, moderate strength increases of ~10% are found in micro-scale specimen when compared to bulk counterparts. This increase in strength is attributed to decreases in the defect density in this small volume. Serrated flow was observed in these micro-scale specimens and was characterized by the initiation and propagation of many shear bands. The differences in strength among micrometer sized specimen is on the order of scatter in the data, and it is not clear if the “smaller is stronger” argument still holds at the micrometer scale for BMG materials. This should be investigated in future studies with a more statistically significant data set.

In W-BMG composites, the matrix phase does show differences in deformation behavior from monolithic specimens. In particular, work hardening is observed and there is some indication of size dependent properties in specimens tested. The matrix material does appear to possess features that are typically beneficial for kinetic energy penetrator materials; high strength and relatively low (when compared to other non-amorphous materials) strain hardening. The foundations have been set in place to use this technique to assess the material properties at the micrometer scale for the design of micro-scale devices and in the development of advanced penetrator materials.

ACKNOWLEDGEMENTS

The authors would like to thank M.D. Uchic for sharing his expertise in microcompression fabrication techniques

and T.A. Waniuk, J. Kajuch and Liquidmetal® Technologies for providing the W-BMG material. Research at the US Army Research Laboratory is supported through the Director’s Research Initiative. This work was performed under the auspices of the Center for Advanced Metallic and Ceramic Systems (CAMCS) at the Johns Hopkins University through Grant No. DAAL01-96-2-0047 and ARMAC-RTP Cooperative Agreement Number DAAD19-01-2-0003. Research at the Oak Ridge National Laboratory SHaRE User Facility was sponsored by the Office of Basic Energy Sciences, U.S. Department of Energy, under contract DE-AC05-00OR22725 with UT-Battelle, LLC.

REFERENCES

- Greer, J.R., Oliver, W.C., and Nix, W.D., 2005: Size dependence of mechanical properties of gold at the micron scale in the absence of strain gradients, *Acta Materialia*, **53**, 1821-1830.
- Hata, S., Kato, T., Fukushige, T., Shimokohbe, A., 2003: Integrated conical linear actuators, *Microelectronic Engineering*, **67-68**, 574-581.
- Kui, H.W., Greer, A.L., and Turnbull, D., 1984: Formation of Bulk Metallic Glass by Fluxing, *Appl. Phys. Lett* **45(6)**, 615-616.
- Lewandowski, J.J., Shazly, M., Shamimi Nouri, A., 2006: Intrinsic and extrinsic toughening of bulk metallic glasses, *Scripta Materialia* **54**, 337-341.
- Lambson, E.F., Lambson, W.A., Macdonald, J.E., Gibbs, M.R.J., Saunders, G.A., Turnbull, D., 1986: Elastic behavior and vibrational anharmonicity of a bulk $\text{Pd}_{40}\text{Ni}_{40}\text{P}_{20}$ Metallic Glass, *Phys Rev B*, Vol **33** No 2, Jan 15 1986.
- Schuster, B.E., Wei, Q., Zhang, H., and Ramesh, K.T., 2006: Microcompression of Nanocrystalline Nickel, *Applied Physics Letters*, **88**, 103112.
- Uchic, M.D., Dimiduk, D.M., Florando, J.N. and Nix, W.D., 2003: Materials Research Society Symposium Proceedings 2003, edited by George, E.P., Inui, H., Mills, and Eggeler, G.; Vol. **753**, BB1.4.
- Uchic, M.D., Dimiduk, D.M., Florando, J.N., and Nix, W.D., 2003: Sample Dimensions Influence Strength and Crystal Plasticity, *Science* **305**, 986-989
- Uchic, M.D. and Dimiduk, D.M., 2005: A methodology to investigate size scale effects in crystalline plasticity using uniaxial compression testing, *Materials Science and Engineering A*, **400-401**, 268-278.
- Wright, W.J., Schwarz, R.B., Nix, W.D., 2001: Localized heating during serrated plastic flow of bulk metallic glasses, *Mat. Sci and Eng* **A319-321**, 229-232.
- Zhang, H., Schuster, B.E., Wei, Q., and Ramesh, K.T., 2006: The design of accurate microcompression experiments, *Scripta Materialia* **54**, 181-186.

NO. OF
COPIES ORGANIZATION

1 DEFENSE TECHNICAL
(PDF INFORMATION CTR
ONLY) DTIC OCA
8725 JOHN J KINGMAN RD
STE 0944
FORT BELVOIR VA 22060-6218

1 US ARMY RSRCH DEV &
ENGRG CMD
SYSTEMS OF SYSTEMS
INTEGRATION
AMSRD SS T
6000 6TH ST STE 100
FORT BELVOIR VA 22060-5608

1 DIRECTOR
US ARMY RESEARCH LAB
IMNE ALC IMS
2800 POWDER MILL RD
ADELPHI MD 20783-1197

3 DIRECTOR
US ARMY RESEARCH LAB
AMSRD ARL CI OK TL
2800 POWDER MILL RD
ADELPHI MD 20783-1197

ABERDEEN PROVING GROUND

1 DIR USARL
AMSRD ARL CI OK TP (BLDG 4600)

NO. OF
COPIES ORGANIZATION

3 DIRECTOR
US ARMY RESEARCH LAB
AMSRD ARL SE RL
M ERVIN
R POLCAWICH
J PULSKAMP
2800 POWDER MILL RD
ADELPHI MD 20783-1197

ABERDEEN PROVING GROUND

7 DIR USARL
AMSRD ARL WM M
R DOWDING
J MCCAULEY
AMSRD ARL WM MB
L KECSKES
H MAUPIN
AMSRD ARL WM TC
R COATES
L MAGNESS
T WRIGHT